Stratigraphy of the Stuhini Group (Upper Triassic) in the Galore Creek area, northwestern British Columbia

Bram I. van Straaten[1], Richard M. Friedman[2], and Alfredo Camacho[3]

[1] British Columbia Geological Survey, Ministry of Energy, Mines and Low Carbon Innovation, Victoria, BC, V8W 9N3

[2] Pacific Centre for Isotopic and Geochemical Research, Department of Earth, Ocean and Atmospheric Sciences, The University of British Columbia, 6339 Stores Road, Vancouver, BC, V6T 1Z4

[3] Manitoba Isotope Research Facility, Department of Earth Sciences, University of Manitoba, 125 Dysart Road, Winnipeg, MB, R3T 2N2

[a] corresponding author: Bram.vanStraaten@gov.bc.ca

Abstract

The 1.4 Bt Galore Creek porphyry Cu-Au-Ag deposit is hosted in, and broadly coeval with, a multi-phase alkalic silica-undersaturated volcano-intrusive complex. Based on stratigraphic studies supplemented by new geochronological data, we subdivide the host Stuhini Group strata (Upper Triassic) into a lower succession and an upper succession. The lower succession (at least ~1.2 km thick) grades upward from reworked intermediate volcanic to sedimentary and mafic volcanic strata. The succession was deposited, at least in part, in a submarine setting, part of the Stuhini arc (~1300 km long) developed along the eastern margin and northern part of Stikinia. The lower succession is abruptly overlain by an upper alkalic volcanic succession (at least ~0.8 km thick). In the eastern part of the study area, the upper succession includes a local biotite-phyric volcanic and reworked volcanic unit, mostly deposited subaqueously. Overlying K-feldspar-phyric volcanic rocks, found throughout the study area, are subaerial deposits as indicated by accretionary lapilli, welded beds, and irregular-shaped bombs. Pseudoleucite-phyric volcanic rocks and pseudoleucite-phyric subvolcanic intrusions are found in the western and central parts of the study area; their depositional setting and relationship to other alkalic units are unclear. We constrain the onset of upper succession alkalic volcanism to 210.26 ±0.17 Ma using high-precision U-Pb zircon and titanite geochronology. The new age is broadly coeval with published ages for mineralogically, texturally, and compositionally similar alkalic silica-undersaturated Galore intrusions (ca. 210-208 Ma) and suggests a short-lived alkalic magmatic event responsible for porphyry Cu-Au-Ag formation. Regionally, the upper alkalic volcanic succession and alkalic silica-undersaturated Galore intrusions are part of a magmatic belt (~155 km long) of small-volume stocks and rare volcanic rocks that orthogonally transects the earlier Stuhini arc. It reflects post-subduction alkalic magmatism and alkalic silica-undersaturated porphyry Cu-Au-Ag deposit formation during the early stages of collision between the Yukon-Tanana and Stikine terranes.

Keywords: Stuhini Group, Late Triassic, stratigraphy, Galore Creek, Copper canyon, porphyry Cu-Au, Galore plutonic suite, silica-undersaturated, alkalic, magmatism, geochronology, Stikinia

1. Introduction

The Galore Creek Cu-Au-Ag deposit is one of several large (>1 Bt) porphyry systems in northwestern British Columbia (Fig. 1) on the traditional lands of the Tahltan First Nation. The deposit is unique with respect to other large deposits in the region in its genetic link to an alkalic silica-undersaturated volcano-intrusive complex, and the presence of silica-deficient hydrothermal alteration (Enns et al., 1995; Logan and Mihalynuk, 2014). The deposit is hosted in the Stuhini Group (Upper Triassic), a volcanic arc succession that is widespread throughout the Stikine terrane (Fig. 1). Herein we present a stratigraphic analysis of the Stuhini Group and show that, in the Galore Creek area, it records an abrupt change from mafic-intermediate arc volcanism to alkalic silica-undersaturated post-arc volcanism. We describe volcano-sedimentary units in the Galore Creek area estimating their thicknesses and lateral variations, provide a preliminary high-precision geochronological determination for the onset of alkalic volcanism, and discuss the tectonic implications.

2. Geological setting
2.1. Regional geology

The Galore Creek area is in the multi-episodic Stikine island arc terrane (Stikinia), in which volcano-sedimentary rocks of the Stikine assemblage (Devonian to Permian) are overlain by the Stuhini Group (Upper Triassic) and the Hazelton Group (uppermost Triassic to Middle Jurassic). These successions are bounded by regional unconformities that mark significant deformation including: 1) poorly characterized Permo-Triassic deformation that affects Paleozoic rocks (Logan and Koyanagi, 1994); 2) latest Triassic deformation that affects Stuhini Group and older strata throughout northwestern British Columbia, and has been attributed to collision between the Yukon-Tanana and Stikine terranes (e.g., Nelson et al., 2022); and 3) a Middle Jurassic fold-and-thrust belt along the northeastern margin of Stikinia, formed due to accretion of Stikinia and intervening Intermontane terranes to Ancestral North America (Mihalynuk et al., 1994; Nelson et al., 2013).

33

Geological Fieldwork 2022, British Columbia Ministry of Energy, Mines and Low Carbon Innovation, British Columbia Geological Survey Paper 2023-01
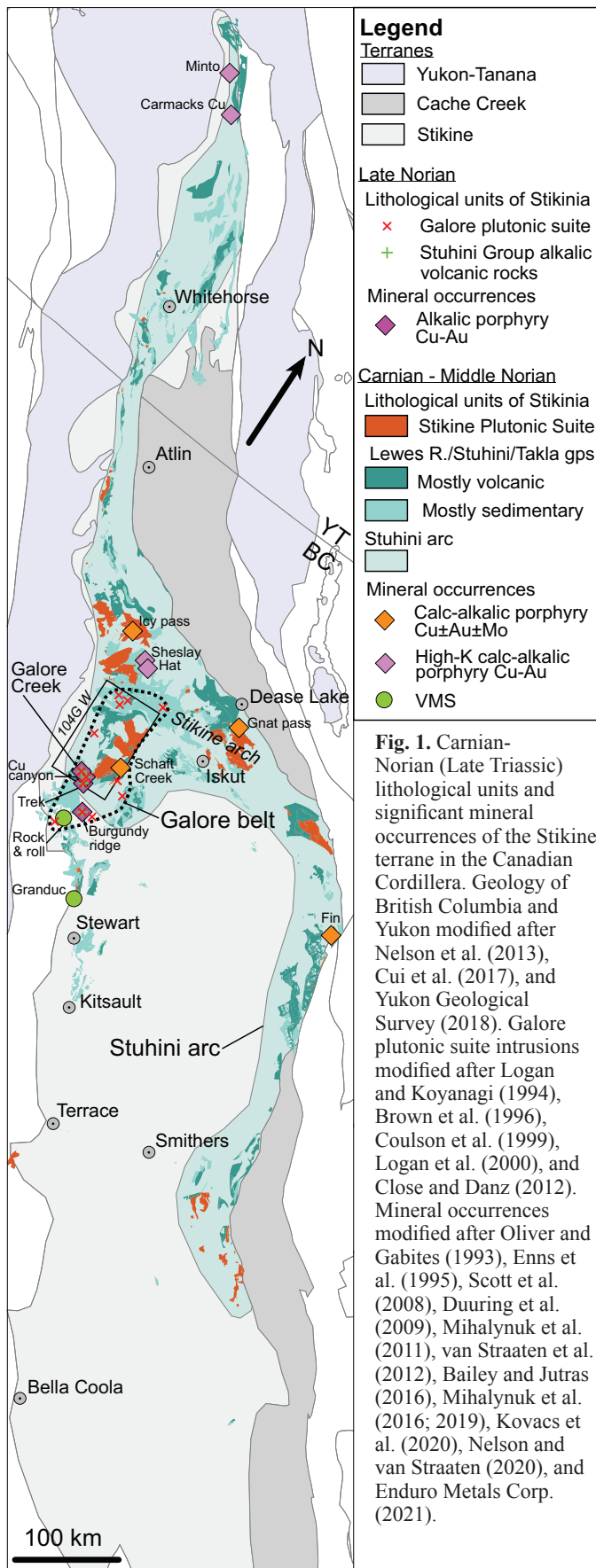
Accretion of Stikinia to inboard terranes and the Ancestral North American margin is recorded by deposition of Bowser Lake Group siliciclastic rocks (Middle Jurassic to mid-Cretaceous) in a foreland basin atop Stikinia (Evenchick et al., 2007). Bowser Lake Group and older rocks are deformed by Cretaceous Skeena fold-and-thrust belt shortening linked to continued convergence between accreted terranes and Ancestral North America (Evenchick et al., 2007).

The main axis of Late Triassic magmatism in Stikinia (hereafter referred to as the Stuhini arc) is defined by thick accumulations of predominantly mafic volcanic strata assigned to the Lewes River Group in Yukon, Stuhini Group in northwestern and central British Columbia, and Takla Group in north-central British Columbia (Fig. 1). These strata are accompanied by ca. 229-216 Ma Stikine Plutonic Suite intrusions. These volcanic and intrusive rocks extend for at least ~1300 km along the eastern margin and northern part of Stikinia (Fig. 1) and have been interpreted as an east-facing arc (Nelson and van Straaten, 2020). Several porphyry Cu±Au±Mo deposits formed along the Stuhini arc (e.g., Schaft Creek, Fig. 1), with VMS deposits developed in the back arc (e.g., Granduc, Fig. 1). Stuhini arc activity terminated in latest Triassic by a collision between northern Stikinia and the Yukon-Tanana terrane. This collision is expressed by: 1) the latest dated Stuhini arc magmatism at ca. 216 Ma (van Straaten et al., 2022); 2) the latest Triassic shortening of the Stuhini Group and older strata throughout northwestern British Columbia (Henderson et al., 1992; Rhys, 1993; Brown et al., 1996; Rees et al., 2015; Nelson et al., 2018); 3) a regional-scale unconformity between the Stuhini and Hazelton groups (e.g., Nelson et al., 2018; 2022); 4) a ca. 9-12 m.y. magmatic gap in the Kitsault, Stewart to Iskut corridor (ca. 216 to 207-204 Ma; Hollis and Bailey, 2013; Hunter and van Straaten, 2020; Campbell, 2021), extending to ca. 31-41 m.y. along the Stikine arch (ca. 216 to 185-175 Ma; Brown et al., 1996; van Straaten et al., 2022); and 5) crustal thickening and burial of the Yukon-Tanana terrane to amphibolite facies in southern Yukon, and coincident ca. 205-194 Ma mid- to lower-crustal magmatism along the Yukon-Tanana - Stikinia suture in southern Yukon (Colpron et al., 2022).

From ca. 210-208 Ma (Mortensen et al., 1995; Logan and Mihalynuk, 2014; Enduro Metals Corp., 2021), a distinct magmatic belt (~155 km long) developed in northwestern Stikinia, orthogonal to the Stuhini arc axis (Fig. 1). This belt is defined by small-volume Galore plutonic suite intrusions of predominantly alkaline affinity and very rare alkalic volcanic rocks. The orientation of the belt, small volume intrusions, localized volcanic rocks and alkalic chemistry suggest that it is a post-subduction feature generated by partial melting of previously subduction-metasomatized sub-arc lithosphere (Nelson and van Straaten, 2020). Recent studies of the collision (Colpron et al., 2022; Nelson et al., 2022) suggest the alkalic magmatism occurred during the early stages of Yukon-Tanana - Stikinia collision.

Fig. 1. Carnian-Norian (Late Triassic) lithological units and significant mineral occurrences of the Stikine terrane in the Canadian Cordillera. Geology of British Columbia and Yukon modified after Nelson et al. (2013), Cui et al. (2017), and Yukon Geological Survey (2018). Galore plutonic suite intrusions modified after Logan and Koyanagi (1994), Brown et al. (1996), Coulson et al. (1999), Logan et al. (2000), and Close and Danz (2012). Mineral occurrences modified after Oliver and Gabites (1993), Enns et al. (1995), Scott et al. (2008), Duuring et al. (2009), Mihalynuk et al. (2011), van Straaten et al. (2012), Bailey and Jutras (2016), Mihalynuk et al. (2016; 2019), Kovacs et al. (2020), Nelson and van Straaten (2020), and Enduro Metals Corp. (2021).

34

Geological Fieldwork 2022, British Columbia Ministry of Energy, Mines and Low Carbon Innovation, British Columbia Geological Survey Paper 2023-01

2.2. Galore Creek area geology

The oldest rocks in the Galore Creek area are in the hanging wall of the west-verging Copper canyon thrust fault and comprise Stikine assemblage limestone (Permian) and fine-grained siliciclastic sedimentary rocks (Lower-Middle Triassic; Logan and Koyanagi, 1994; Fig. 2). Elsewhere, the area is underlain by Stuhini Group volcano-sedimentary rocks (Upper Triassic). Logan and Koyanagi (1994) subdivided the Stuhini Group into: 1) a lower unit of subalkaline hornblende-bearing basaltic andesite and sedimentary equivalent wacke, turbidite, and conglomerate; 2) a middle unit of subalkaline to alkaline augite-porphyritic basalt, and sedimentary and epiclastic rocks

with predominantly pyroxene; and 3) an uppermost unit of alkaline orthoclase- and pseudoleucite-bearing shoshonitic basalt, tuff, and epiclastic rocks. Stuhini Group strata are cut by foid syenite, alkali-feldspar syenite, syenite, monzonite, monzodiorite, and rare quartz syenite of the Galore intrusions (part of the Galore plutonic suite) that are K-feldspar and/or pseudoleucite porphyritic and less commonly equigranular (Enns et al., 1995; Fig. 2). The age range of alkalic silica-undersaturated Galore intrusions has been difficult to establish due to a general lack of zircon and thermal resetting. It is broadly constrained by a 210 ±1 Ma U-Pb titanite and K-feldspar age for an early syn-mineralization K-feldspar and
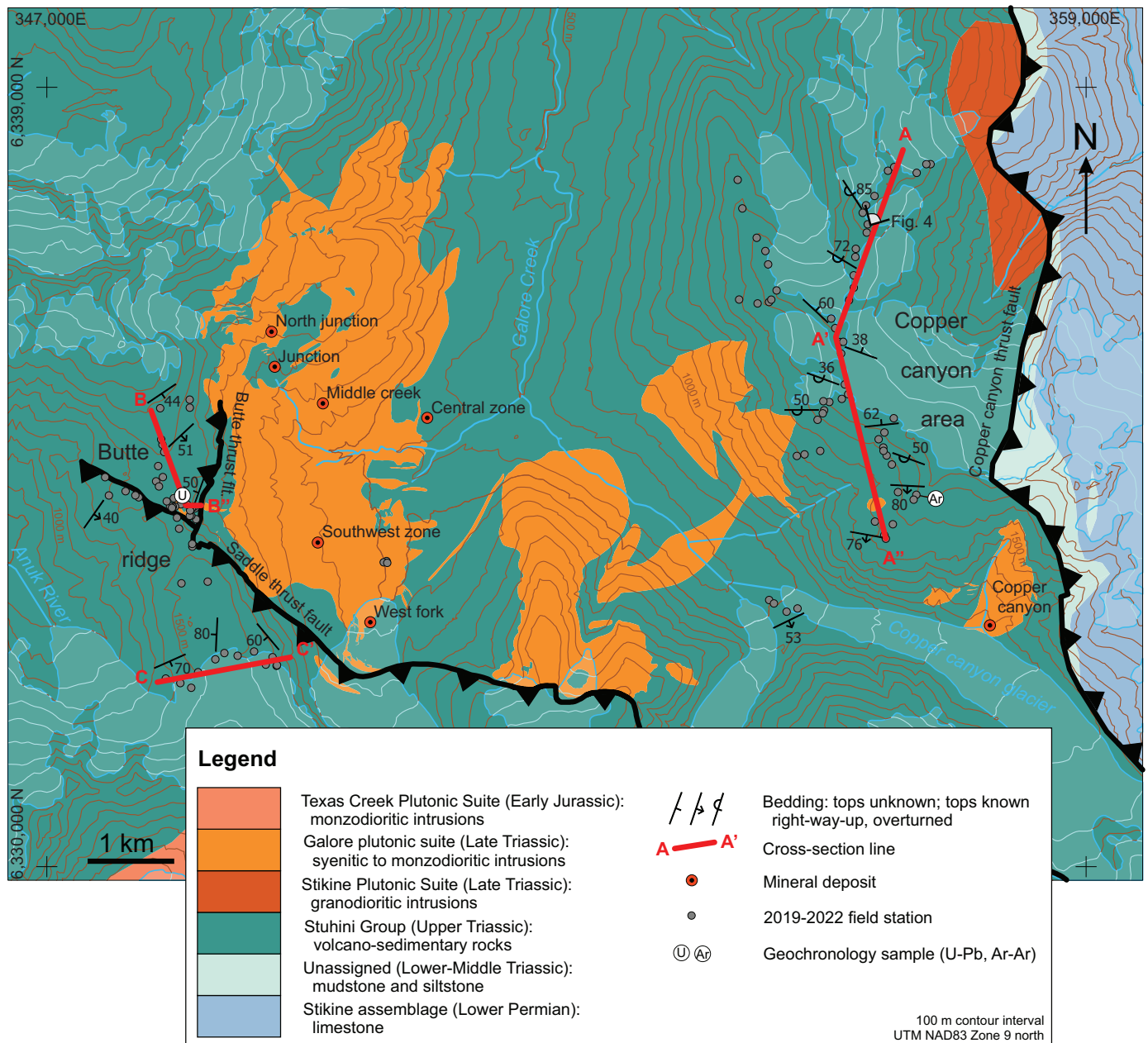
Fig. 2. Geology of the Galore Creek area (modified after Logan et al., 1993a, b; Cui et al., 2017). Galore intrusions, Butte and Saddle thrust faults after Prince (2020). UTM coordinates here and throughout this paper are in NAD83 zone 9 north.

35

Geological Fieldwork 2022, British Columbia Ministry of Energy, Mines and Low Carbon Innovation, British Columbia Geological Survey Paper 2023-01

pseudoleucite porphyritic syenite intrusion (Mortensen et al., 1995) and a 208.5 ±0.8 Ma U-Pb titanite age for a K-feldspar porphyritic biotite quartz syenite plug (Logan and Mihalynuk, 2014) interpreted by Enns et al. (1995) as the youngest phase of the Galore intrusions.

Compared to porphyry deposits worldwide, Galore Creek represents a unique alkalic silica-undersaturated endmember (Lang et al., 1995). Chalcopyrite ±bornite mineralization is hosted in Stuhini Group strata, breccia bodies, and early- to syn-mineralization Galore intrusions, and is accompanied by silica-deficient hydrothermal alteration including K-feldspar, biotite, garnet and anhydrite (Enns et al., 1995; Byrne and Tosdal, 2014; Micko et al., 2014). At least two mineralizing episodes are interpreted, with large volume orthoclase megacrystic syenite intrusions mostly late- to post-mineral (Enns et al., 1995; Schwab et al., 2008; Byrne and Tosdal, 2014; Micko et al., 2014).The Galore Creek district contains NI 43-101 compliant mineral resources (Measured, Indicated, and Inferred) of 1466 Mt containing 15 Blbs Cu, 13 Moz Au and 205 Moz Ag across six different deposits (Central zone, Southwest zone, Junction/North Junction, West fork, Middle creek and Copper canyon; Table 1, Fig. 2; Hatch Ltd. et al., 2005; Teck Resources Limited, 2019). Mineral resource estimates are currently being updated as part of a prefeasibility study carried out by Galore Creek Mining Corporation, a 50/50 partnership between Teck Resources Limited and Newmont Corporation.

Fig. 4). Consistent southwest younging directions <100 m on either side of the folds imply they are minor parasitic folds (Figs. 3a, 4). Although other unrecognized folds may result in overestimation of the calculated thickness of units, they unlikely affect the interpreted stratigraphic superposition presented below (see Section 4). Two faults, one low angle and the other high angle, are interpreted in recessive zones surrounded by wall rock with a well-developed fault-parallel spaced fracture cleavage. Stratigraphic offsets suggest an apparent reverse south- to southwest-vergent sense for both. The northern half of the cross section displays consistently overturned steeply northeast-dipping strata, except one right-way-up very steeply west-southwest-dipping bedding measurement. Bedding attitudes shallow towards the middle of the cross section. Slightly farther south in a fault-bounded panel, one measurement shows an overturned shallow north-northeast dip. The southern half of the cross-section shows largely overturned moderately north-northeast-dipping strata with rare right-way-up steeply south-southwest dipping strata. Stereonet analysis shows that all poles to overturned and inferred overturned bedding planes cluster in the southwest quadrant, whereas poles to right-way-up bedding planes are in the northeast quadrant (Fig. 5a). The variation in bedding attitudes is attributed to fault rotation, minor asymmetric folds, original non-horizontal deposition of volcanic strata, surface processes such as frost-heave, and measurement errors. Tectonic foliation is absent to weak outside of the fault zones noted above.

Table 1. Total NI 43-101 compliant mineral resources in the Galore Creek area. Galore Creek estimates from Teck Resources Limited (2019), Copper canyon estimates from Hatch Ltd. et al. (2005).

Category	Zone	Mt	Cu (%)	Au (g/t)	Ag (g/t)	Cu (Blbs)	Au (Moz)	Ag (Moz)
Measured	Galore	256.8	0.72	0.36	5.8	4.06	3.00	47.80
Indicated	Galore	846.7	0.39	0.23	3.7	7.27	6.26	102.05
Inferred	Galore	198.1	0.27	0.21	2.7	2.95	1.34	16.88
Inferred	Cu canyon	164.8	0.35	0.54	7.2	1.16	2.86	37.91
Total		**1466.4**	**-**	**-**	**-**	**15.43**	**13.46**	**204.63**

3. Study area structure and stratigraphic superposition

In this study we establish the Stuhini Group (Upper Triassic) stratigraphy in the Galore Creek area based on detailed field studies at three locations; one northwest of the Copper canyon deposit and two on Butte ridge (between the headwaters of the Anuk River and Galore Creek; Figs. 2, 3).

3.1. Copper canyon area

Stuhini Group strata throughout the Copper canyon area consistently young towards the southwest and south (Section A-A'-A'', Fig. 3a) although largely coherent mafic volcanic or subvolcanic rocks in the far north lack bedding measurements and younging indicators. Along the entire cross section line, we observed only one 0.5 m-scale tight synform and a nearby several m-scale open asymmetrical z-fold (looking north;

3.2. Butte ridge north

The northwest end of Butte ridge exposes moderately southeast dipping right-way-up Stuhini Group strata (Section B-B'-B'', Fig. 3b) with at least one ~140 m-scale asymmetric open s-fold (looking north). The succession steepens towards B'. In the northeast, between B' and B'', steeply west-dipping strata lack way up indicators. Here, the upper part of a volcanic succession (uTrSvc.gal) contains an s-fold (looking north); farther east near the volcanic-sedimentary contact we noted z-folds (looking north; Fig. 3b). Sedimentary clasts in the volcanic rocks immediately above the volcanic-sedimentary contact may suggest this part of the succession is right-way-up. If so, the z- and s-fold geometries suggest the presence of an ~60 m-scale isoclinal syncline. The change in attitudes and rock types at B' have been tentatively interpreted to mark a fault.

36

Geological Fieldwork 2022, British Columbia Ministry of Energy, Mines and Low Carbon Innovation, British Columbia Geological Survey Paper 2023-01
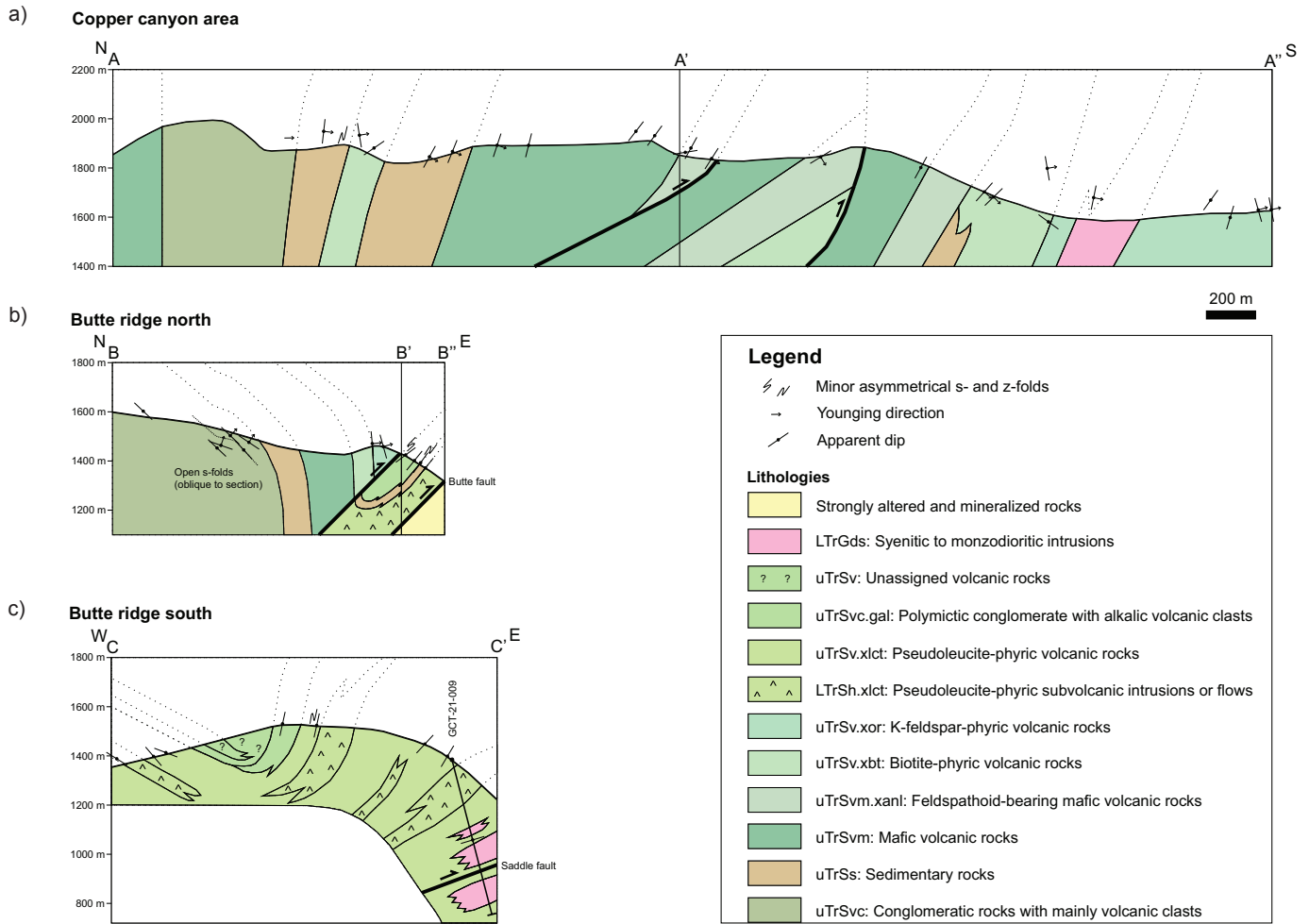
Fig. 3. Schematic vertical cross sections. **a)** Copper canyon area. **b)** North end of Butte ridge. **c)** South end of Butte ridge.
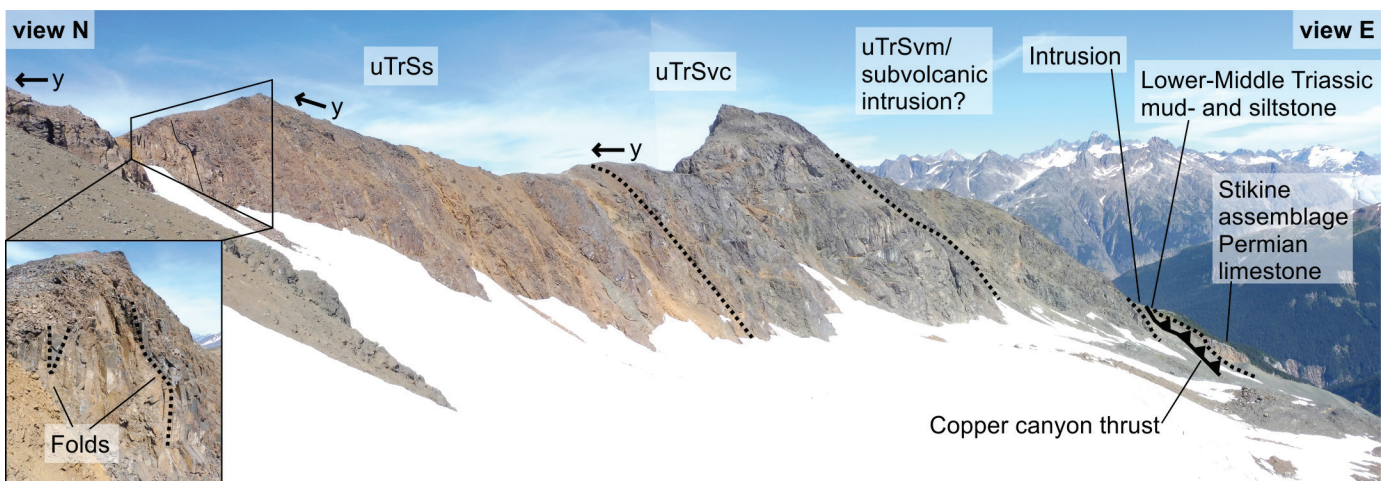
Fig. 4. Panoramic view of alpine ridge in Copper canyon area showing Stuhini Group units in the footwall of the Copper canyon thrust fault. Looking north to east (UTM 356478E–6337417N, see Fig. 2 for location). Inset shows 0.5 m-scale tight synform and a several m-scale open asymmetrical z-fold (looking north). y = younging direction.

37

Geological Fieldwork 2022, British Columbia Ministry of Energy, Mines and Low Carbon Innovation, British Columbia Geological Survey Paper 2023-01

A) Cu canyon area

n=33

Defined / Inferred

- ● ● S0, right-way-up
- ● ● S0, tops unknown
- ○ ○ S0, overturned
- ● S1
- ● F1
- ■ β

B) Butte north

n=47

C) Butte south

n=11

	10
	8
	6
	4
	2

Kamb contours in standard deviations
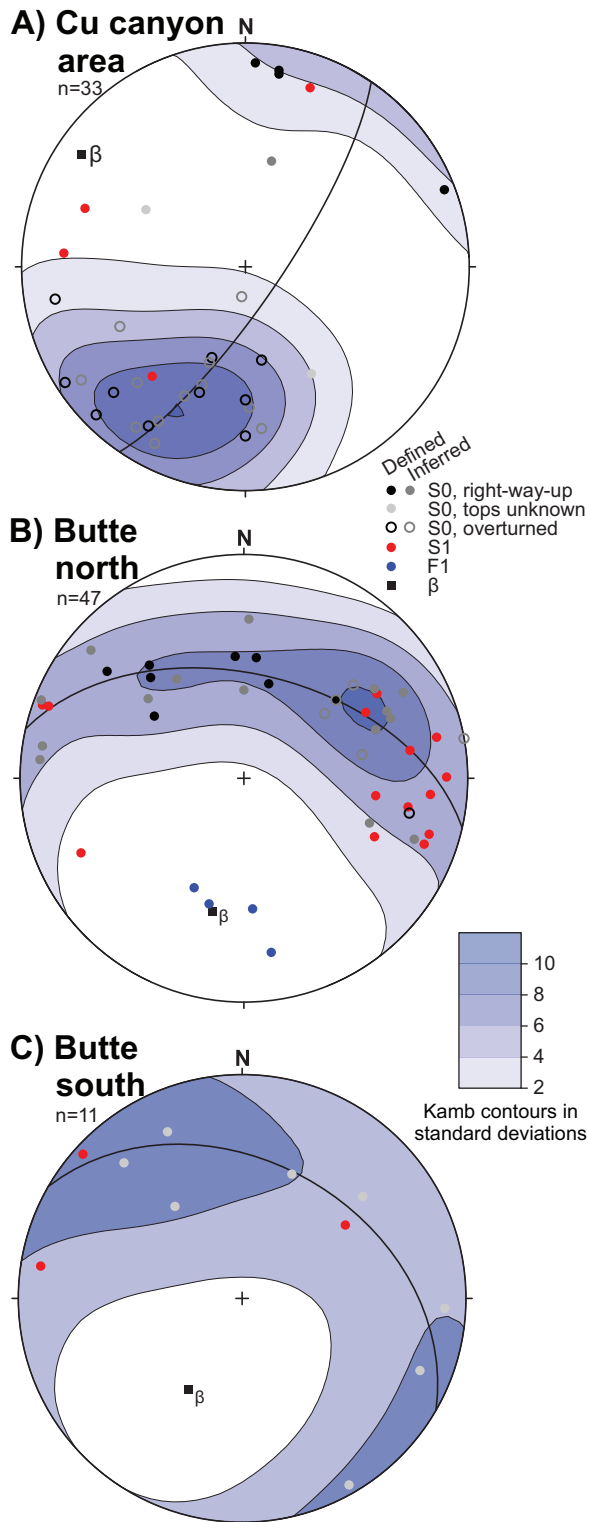
Fig. 5. Stereographic projections showing poles to bedding (S0, contoured), poles to foliation (S1) and fold axes (F1) along **a)** cross-section A-A'-A''; **b)** B-B'-B''; and **c)** C-C'. Lower hemisphere equal area projections were produced using Stereonet 11, where known and inferred overturned bedding planes are shown with negative poles (poles to overturned planes point upward into the upper hemisphere and are plotted in the lower hemisphere; Allmendinger et al., 2013; Cardozo and Allmendinger, 2013). Calculated best fit fold axes (β) are 304°/13° in a), 193°/39° in b), and 210°/51° in c).

The interpreted syncline is in the immediate hanging wall of the Butte thrust fault (Fig. 3b), which juxtaposes largely unaltered rocks with altered and mineralized rocks in the Galore Creek valley (Schwab et al., 2008; Prince, 2020). Stereonet analysis shows a moderately south-southwest plunging fold axis, similar to two measured fold axes and two fold axes calculated from bedding measurements of outcrop-scale folds (Fig. 5b). The entire area displays a steeply west-dipping flattening fabric (Figs. 5b, 6; see Johnston et al., 2023).

3.3. Butte ridge south

At the south end of Butte ridge, bedding measurements are limited and younging indicators were not observed. Southeast dipping Stuhini Group strata in the west and broadly west dipping strata in the east define a possible synform (Section C-C', Fig. 3c). One z-fold (looking north), observed in the east, supports this interpretation. At depth towards the east in diamond drill hole GCT-21-009, oriented core data shows that bedding shallows to a gentle southwest dip before intersecting a fault correlated with the Saddle thrust fault (Prince, 2020). Stereonet analysis shows a moderately southwest-plunging fold axis (Fig. 5c). For the purpose of constructing a stratigraphic column we assume the strata in the moderately plunging fold are right-way-up (see Section 4). Given the limited bedding measurements and lack of way-up indicators, more major folds could be in this area, which would result in overestimation of unit thicknesses. The entire area displays a steeply dipping west- to northwest-dipping flattening fabric (see Johnston et al., 2023).

4. Geological units

All stratified units and subvolcanic intrusions described below are part of the Stuhini Group (Upper Triassic), which we have subdivided into a lower intermediate to mafic volcano-sedimentary succession, and an upper alkalic volcanic succession (Fig. 7). The vertical arrangement of units, from
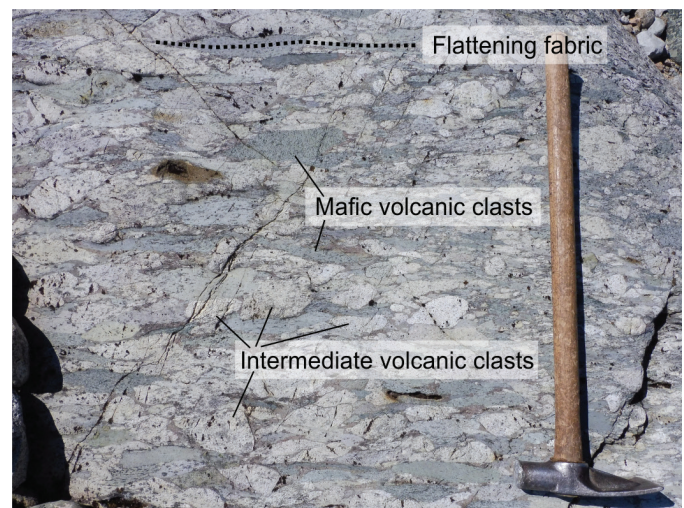
Fig. 6. Foliated polymictic conglomerate with light-toned intermediate volcanic clasts and medium green mafic volcanic clasts in a sandy matrix at north end of Butte ridge, unit uTrSvc (UTM 348320E–6334933N).

38

Geological Fieldwork 2022, British Columbia Ministry of Energy, Mines and Low Carbon Innovation, British Columbia Geological Survey Paper 2023-01
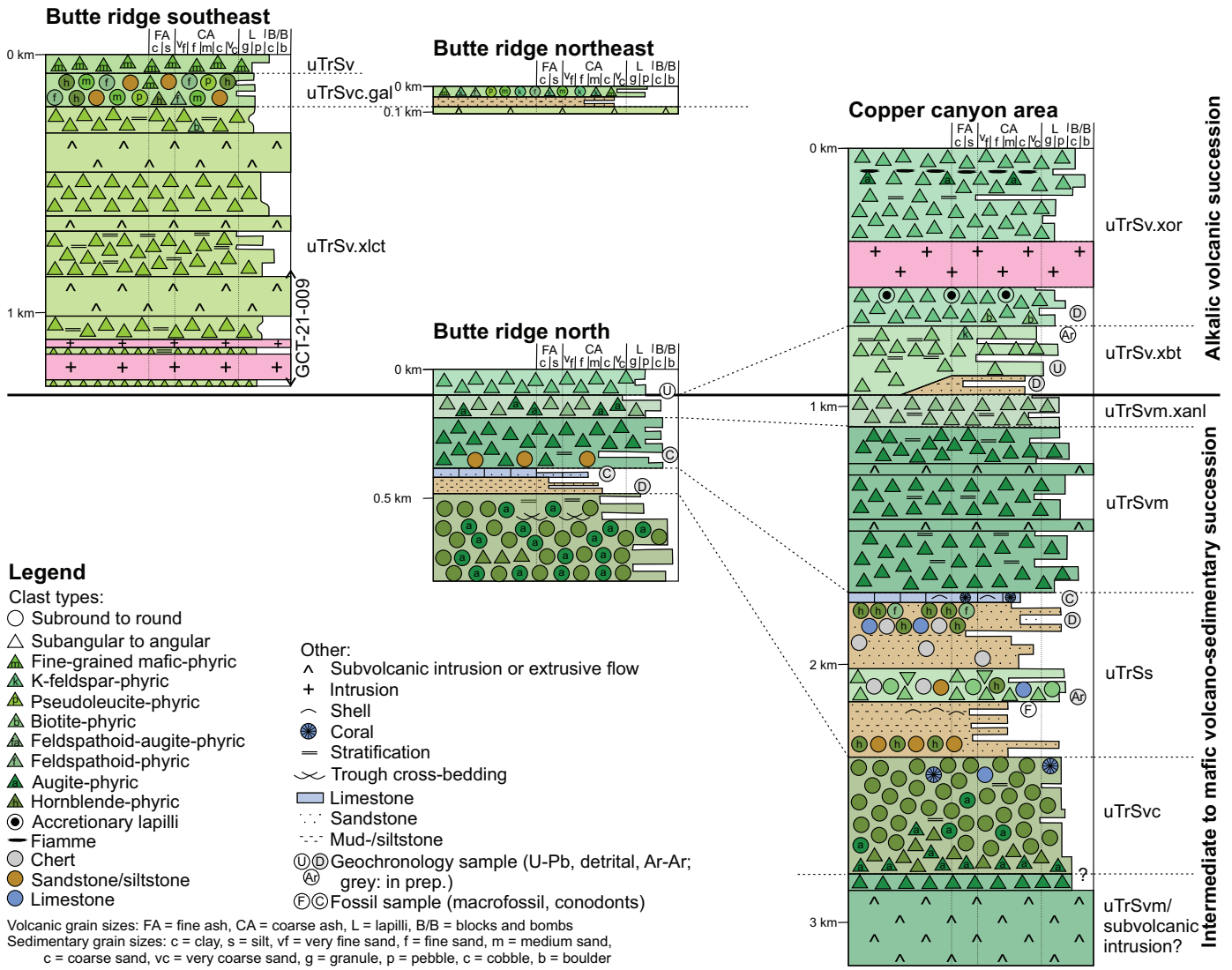
Fig. 7. Schematic stratigraphic sections for the southeast end of Butte ridge, northeast end of Butte ridge, north end of Butte ridge, and Copper canyon area. Stratigraphic units labelled on right-hand side of stratigraphic columns. See Figure 3 for colour legend of rock types.

bottom to top, was determined from observations presented above. Unit thicknesses were calculated by measuring the distance perpendicular to strike between stations and correcting for bedding dip, elevation change, and the presence of folds. Stuhini Group units are cut by Galore intrusions, part of the Galore plutonic suite (Late Triassic).

4.1. Stuhini Group (Upper Triassic)
4.1.1. Lower intermediate to mafic volcano-sedimentary succession

The lower succession comprises a conglomeratic unit with mainly volcanic clasts, a finer grained sedimentary unit, a mafic volcanic unit, and a feldspathoid-bearing mafic volcanic unit; all units are exposed in the Copper canyon area and at the north end of Butte ridge (Figs. 3a, b, and 7).

At the base of the section is a conglomeratic unit (uTrSvc) with light-toned hornblende-phyric intermediate volcanic

clasts and generally lesser medium green augite-phyric mafic volcanic clasts (Fig. 6). Metre-scale beds of conglomerate are interlayered with dm-scale beds of medium- to very coarse-grained sandstone and pebbly sandstone containing mainly volcanic fragments (Fig. 8). Minor intermediate and mafic volcanic rocks are locally observed. At Butte ridge, the unit fines upward from boulder conglomerate to pebble conglomerate, and the proportion of sandstone increases up section (Fig. 7); trough cross-bedding was observed near the top of the unit. In the Copper canyon area, a succession of mafic coherent rocks and minor mafic fragmental volcanic rocks is northeast of the polymictic conglomerate unit (Figs. 3a, 4 and 7). A lack of bedding measurements, way-up criteria, and the generally coherent nature of these rocks precludes a straightforward interpretation of their stratigraphic position. These rocks could represent a unit of mafic volcanic rocks stratigraphically below uTrSvc, or a relatively thin interbed of mafic volcanic rocks and

39

Geological Fieldwork 2022, British Columbia Ministry of Energy, Mines and Low Carbon Innovation, British Columbia Geological Survey Paper 2023-01

Fig. 8. Conglomerate and pebbly sandstone with well-rounded predominantly light-toned intermediate volcanic clasts, Copper Canyon area, unit uTrSvc (UTM 356557E–6337744N).

Fig. 9. a) Laminated to dm-scale bedded sandstone and siltstone, unit uTrSs (UTM 348339E–6334499N). **b)** Bivalve *Monotis (Pacimonotis) subcircularis* Gabb 1864 (C. McRoberts, pers. comm., 2022) in sedimentary unit (22BvS-19-177, UTM 356420E–6337551N).

a thick mafic subvolcanic intrusion within uTrSvc. The fining-upward trend observed at Butte ridge continues in overlying unit uTrSs (Fig. 7), suggesting that the upper contact of unit uTrSvc is gradational.

The conglomeratic unit (uTrSvc) is overlain by a sedimentary unit (uTrSs; Figs. 3a, b, 4 and 7) in which interstratified fine- to very coarse-grained sandstone and siltstone predominate (Fig. 9a). Coarser grained sandstone contains abundant angular feldspar crystals, locally common light-toned microphenocrystic (likely intermediate) volcanic clasts, and ~2% quartz crystals. Minor conglomerate interbeds contain hornblende-phyric intermediate volcanic clasts, sedimentary rip-up clasts, chert clasts, limestone clasts and locally fine-grained white feldspathoid-phyric volcanic clasts. Bivalve imprints in the Copper canyon area (Fig. 9b) have been identified as *Monotis (Pacimonotis) subcircularis* Gabb 1864, a key index species of the Upper Norian Gnomohalorites cordilleranus ammonoid zone (C. McRoberts, pers. comm., 2022). Minor lime mudstone, limestone contaminated by siliciclastic sand and rare packstone is at or near the top of the unit. In the Copper canyon area, solitary corals are present in packstone and as reworked clasts in overlying sandstone. Also in the Copper canyon area, the unit contains an interval of biotite-phyric volcanic rocks and polymictic conglomerate with biotite-phyric volcanic clasts, chert clasts, sandstone/siltstone clasts, hornblende-phyric intermediate volcanic clasts and limestone clasts (Fig. 7). Interbedded mafic volcanic rocks, sandstone, siltstone, and lime mudstone at the base of the overlying mafic volcanic unit (uTrSvm) in the Copper canyon area suggest that the contact between uTrSs and uTrSvm is gradational. At Butte ridge, the contact with the overlying mafic volcanic unit (uTrSvm) is sharp.

A mafic volcanic unit (uTrSvm) overlies the sedimentary unit (uTrSs). It consists of lapillistone, tuff breccia, volcanic breccia,

lesser coarse crystal tuff, and fine tuff. Volcanic clasts contain 15-30% equant augite phenocrysts (0.1-3 mm) and, locally, minor plagioclase phenocrysts and/or amygdules. Volcanic clasts commonly have smooth to lobate edges (Fig. 10) suggesting minimal reworking. At Butte ridge are very rare beds of volcanic-derived sandstone and limestone contaminated by crystal tuff or siliciclastic sand. Augite-phyric amygdaloidal coherent intervals, with up to 30-40% augite phenocrysts (up to 5 mm) and commonly with tubular vesicles represent sills and dikes, although some may be flows. At the north end of Butte ridge, volcanic rocks assigned to the overlying feldspathoid-bearing mafic volcanic unit (uTrSvm.xanl) contain both augite-phyric and feldspathoid-augite-phyric clasts, suggesting that the upward transition from unit uTrSvm is gradational.

A feldspathoid-bearing mafic volcanic unit (uTrSvm.xanl) overlies the mafic volcanic unit (uTrSvm). In the Copper canyon area, lapillistone, crystal tuff and volcanic breccia contain volcanic clasts up to 1 m with 10% white feldspathoid (0.2-2 mm) and 15% augite (1-2 mm) phenocrysts (Fig. 11). Based on the fine-grained nature of the feldspathoid and its occurrence in mafic rocks, it is interpreted as analcime. In the Copper canyon area, a biotite-phyric volcanic unit (uTrSv.

40

Geological Fieldwork 2022, British Columbia Ministry of Energy, Mines and Low Carbon Innovation, British Columbia Geological Survey Paper 2023-01
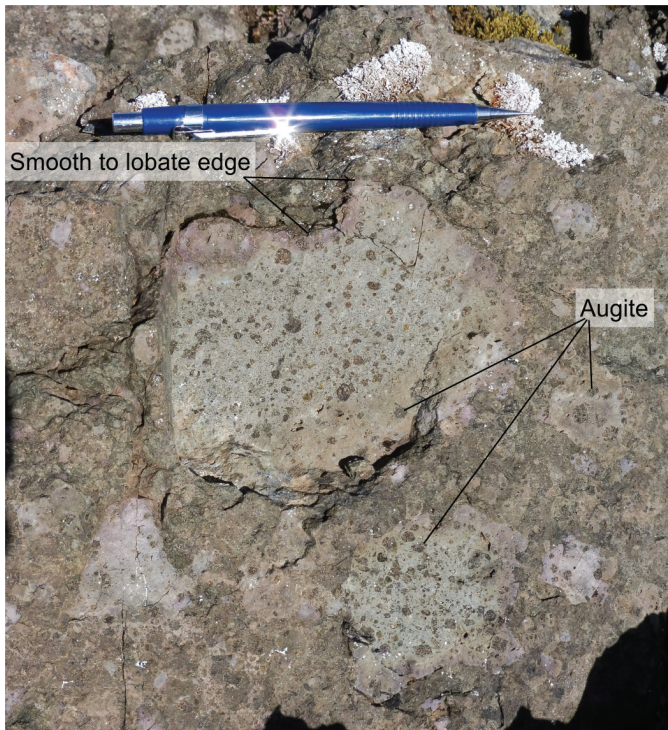
Fig. 10. Mafic tuff breccia with augite-phyric volcanic clasts with smooth to lobate edges, unit uTrSvm (UTM 356316E–6336829N).

xbt) of the upper succession overlies the feldspathoid-bearing mafic volcanic unit but is separated by a 2-metre covered interval. In the absence of evidence of a fault, we assume an abrupt stratigraphic contact. At the north end of Butte ridge, the K-feldspar-phyric volcanic unit (uTrSv.xor) of the upper succession overlies unit uTrSvm.xanl. In this case, the contact is exposed and sharp (Fig. 12), which we take as marking an abrupt stratigraphic transition between the lower and upper succession.

4.1.2. Upper alkalic volcanic succession

The upper alkalic volcanic succession can be subdivided into a biotite-phyric volcanic unit (uTrSv.xbt), a K-feldspar-phyric volcanic unit (uTrSv.xor), pseudoleucite-phyric volcanic and subvolcanic units (uTrSv.xlct and LTrSh.xlct), and a polymictic conglomerate unit with alkalic volcanic clasts (uTrSvc.gal; Fig. 7). The biotite-phyric volcanic unit was only observed in the Copper canyon area. The K-feldspar phyric volcanic unit is exposed in the Copper canyon area and at the north end of Butte ridge. The pseudoleucite-phyric units and polymictic conglomerate unit are only found on Butte ridge (Fig. 3). The stratigraphic position of the pseudoleucite-phyric units and polymictic conglomerate unit relative to the other alkalic volcanic units is poorly constrained.

The biotite-phyric volcanic unit (uTrSv.xbt) consist of laminated to m-scale bedded maroon and green coarse crystal tuff, lapilli-tuff, lapillistone and fine tuff with biotite-phyric volcanic clasts and common free biotite crystals (Fig. 13). Interbeds of biotite-rich volcanic sandstone and volcanic
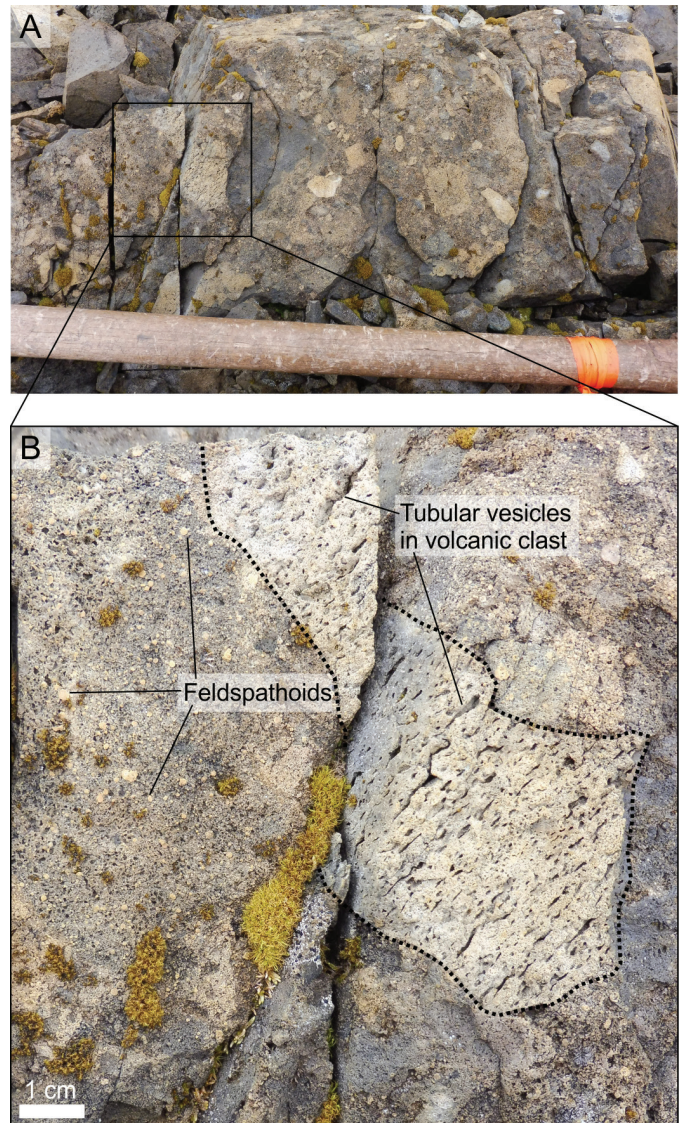
Fig. 11. a) Lapillistone. **b)** close up of a) showing subangular volcanic clasts containing fine-grained white feldspathoids, augite, and rare tubular vesicles, unit uTrSvm.xanl (UTM 355296E–6337109N).

siltstone are locally common and contain rare soft-sediment deformation structures. Farther east (shown at depth on Fig. 3a), the base of the unit comprises laminated to dm-scale bedded siltstone, medium- to very coarse-grained sandstone, and lesser m-scale beds of lapillistone. Siliciclastic strata show fining upward sandstone to siltstone couplets with common basal flames, scours, and load casts. A similar maroon tuff to lapillistone unit with biotite-phyric clasts at the toe of the Copper canyon glacier locally contains accretionary lapilli near its top contact. In the Copper canyon area and at the toe of the Copper canyon glacier (Fig. 2), the biotite-phyric volcanic unit is gradationally overlain by a K-feldspar-phyric volcanic unit (uTrSv.xor), with the biotite crystal content decreasing and the K-feldspar crystal content increasing across the contact (Fig. 7).

41

Geological Fieldwork 2022, British Columbia Ministry of Energy, Mines and Low Carbon Innovation, British Columbia Geological Survey Paper 2023-01
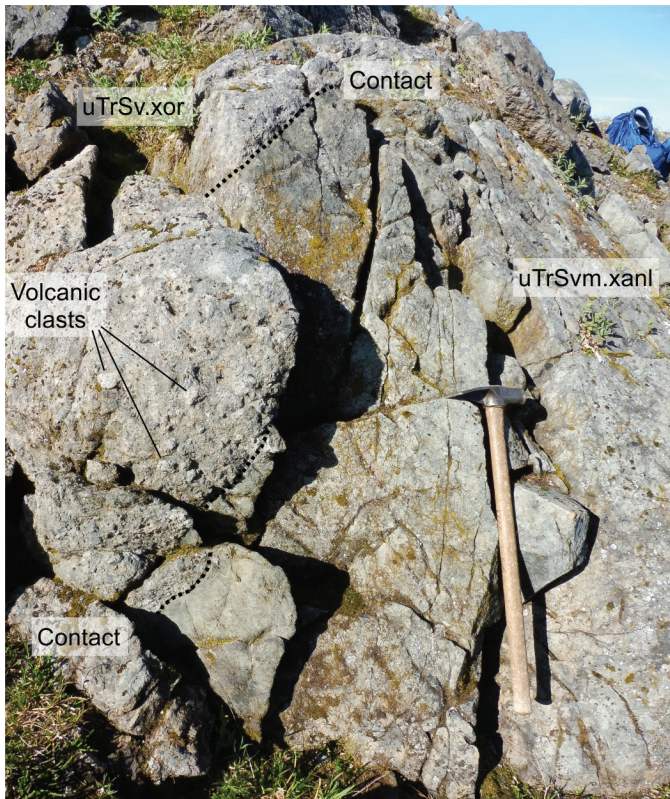
Fig. 12. Sharp basal contact of K-feldspar-phyric volcanic unit (uTrSv.xor) with underlying feldspathoid-bearing mafic volcanic unit (uTrSvm.xanl), north end of Butte ridge (UTM 348453E–6334157N).

Fig. 13. Laminated to dm-scale bedded crystal tuff and lapilli-tuff with biotite crystals (unit uTrSv.xbt) (UTM 355975E–6335269N).

The K-feldspar-phyric volcanic unit (uTrSv.xor) comprises crudely interstratified lapilli-tuff, tuff, lapillistone, tuff breccia, and volcanic breccia containing predominantly K-feldspar-phyric clasts and free blocky to tabular K-feldspar crystals up to 2-5 cm long (Fig. 14a). Volcanic clasts show a wide range in K-feldspar phenocryst abundance, size, and shape. Accretionary lapilli were locally observed near the bottom of the unit in the Copper canyon area (Fig. 14b). The unit contains minor welded lapilli tuff with sparsely K-feldspar-phyric fiamme in the Copper canyon area and at the north end of Butte ridge (Fig. 14c). In the Copper canyon area, rare tuff breccia
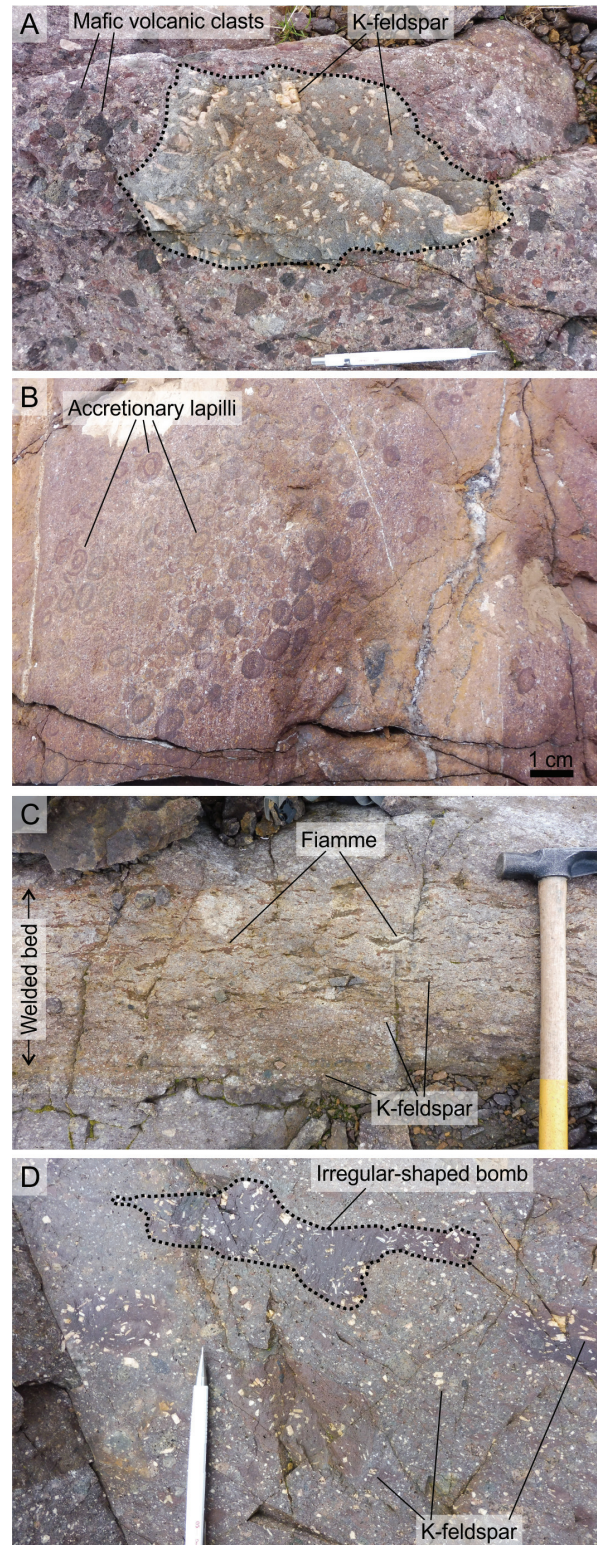
Fig. 14. K-feldspar-phyric volcanic unit (uTrSv.xor). **a)** Tuff breccia with K-feldspar-phyric volcanic clasts, dark-toned augite-plagioclase-phyric mafic volcanic clasts and maroon to grey fine-grained volcanic clasts (UTM 356670E–6333826N). **b)** Lapilli-tuff with accretionary lapilli (UTM 356828E–6334325). **c)** Welded lapilli-tuff with sparsely K-feldspar-phyric fiamme (same UTM as a). **d)** Lapillistone with sparsely K-feldspar-phyric volcanic bombs with lobate outlines (same UTM as a).

42

Geological Fieldwork 2022, British Columbia Ministry of Energy, Mines and Low Carbon Innovation, British Columbia Geological Survey Paper 2023-01

with K-feldspar-phyric volcanic clasts and augite-plagioclase-phyric clasts, both with subangular shapes to irregular lobate borders, suggests coeval eruption of alkalic and mafic magma. Locally in the Copper canyon area are sparsely K-feldspar-phyric elongate volcanic bombs with irregular lobate borders (Fig. 14d). Welding textures, accretionary lapilli, and irregular-shaped volcanic bombs all suggest primary pyroclastic subaerial deposition.

A pseudoleucite-phyric volcanic unit (uTrSv.xlct) is exposed on the southern and eastern parts of Butte ridge (Figs. 3c, 7), but contact relationships with units described above were not observed. The unit comprises lapillistone to lapilli-tuff, lesser tuff breccia, and minor laminated to cm-scale bedded fine tuff and coarse crystal tuff. The rocks contain clast- to matrix-supported light to medium grey to greenish-grey pseudoleucite-phyric volcanic clasts, light to medium grey to greenish grey aphyric volcanic clasts and common free pseudoleucite crystals in an ash matrix (Fig. 15a). Crude stratification is defined by slight variations in clast size and rare tuff layers. Irregular- to amoeboid-shaped pseudoleucite-phyric clasts are locally common. Massive intervals with abundant broken pseudoleucite crystals (Fig. 15b) are likely fragmental in origin; the uniform appearance of these intervals may be due to welding or alteration of matrix. The unit contains minor pseudoleucite-phyric coherent intervals similar to unit LTrSh.xlct described below.

Pseudoleucite-phyric coherent rocks (unit LTrSh.xlct) are common on the southern, eastern, and northeastern parts of Butte ridge (Figs. 3b, c and 7). They generally contain 15-35% zoned pseudoleucite phenocrysts (1-5 cm; Fig. 15c); crystals are locally flattened and rarely broken. Abrupt contacts, locally sharp and clearly intrusive, suggest these are mostly subvolcanic intrusions cutting units uTrSv.xlct and uTrSvc.gal, although some coherent intervals could also be extrusive lava flows.

A polymictic conglomerate unit with alkalic volcanic clasts (uTrSvc.gal) occurs on the southern and northeastern parts of Butte ridge. At the south end of Butte ridge, polymictic conglomerate is interbedded with lesser sandstone to coarse crystal tuff laminae, beds, and lenses (Fig. 16). The pebble to rare cobble conglomerate contains subangular to subrounded fine-grained feldspathoid-phyric volcanic clasts, hornblende-phyric intermediate volcanic clasts, green fine-grained volcanic clasts, pseudoleucite-phyric volcanic clasts, stratified crystal tuff to sandstone clasts, and very rare chert and limestone clasts. At the northeast end of Butte ridge, green laminated to cm-scale bedded volcanic-derived sandstone transitions gradationally westward into alternating interbeds of: 1) lapillistone to lapilli-tuff with volcanic clasts containing 10-15% mostly equant mafic phenocrysts (0.5-1.5 mm); 2) lapillistone to lapilli-tuff with volcanic clasts containing tabular K-feldspar phenocrysts; 3) polymictic pebble conglomerate containing predominantly volcanic clasts similar to 1) and 2) above and sparser clasts with 15% white feldspathoid (0.2-3 mm) phenocrysts, clasts
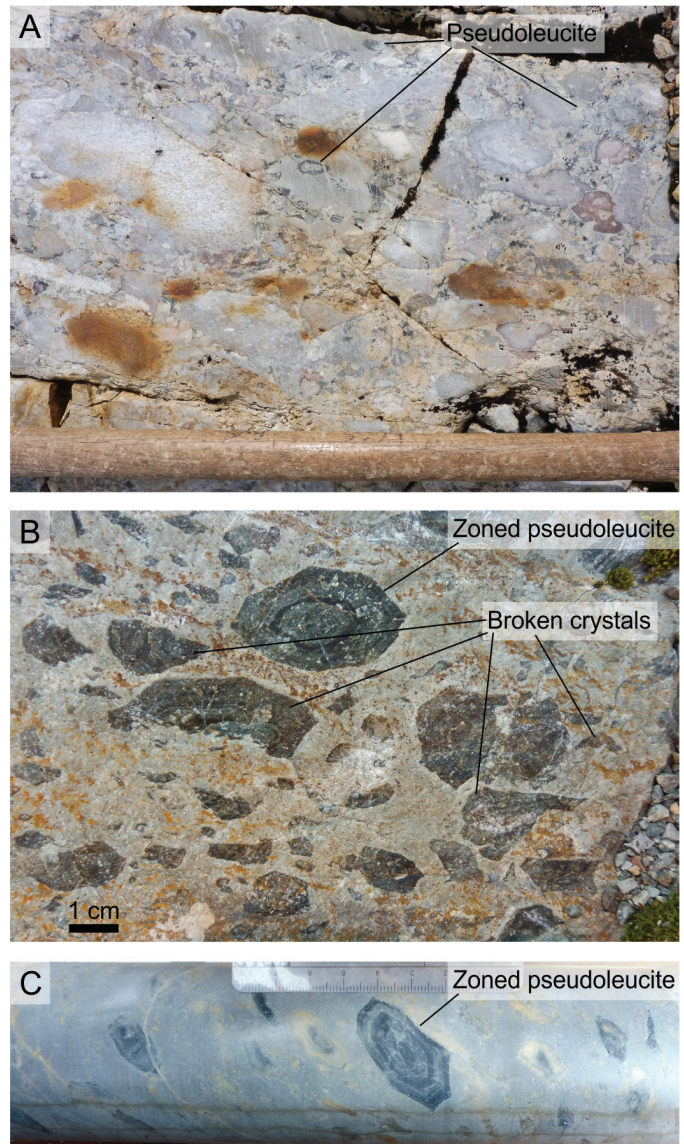
Fig. 15. Pseudoleucite-phyric volcanic and subvolcanic units (uTrSv.xlct, LTrSh.xlct). **a)** Tuff breccia with pseudoleucite-phyric and aphyric volcanic clasts (349393E–6332484N). **b)** Massive rock with abundant broken pseudoleucite crystals (349657E–6332326N). **c)** Coherent rock with coarse pseudoleucite phenocrysts (DDH GCT-21-009, UTM 349652E–6332319N).

with pseudoleucite phenocrysts, and clasts with feldspathoid and K-feldspar phenocrysts; and 4) volcanic-derived sandstone to crystal tuff (Figs. 3b, 7). Common stratified green siltstone to sandstone clasts in the basal volcanic rocks suggest the succession is right-way-up.

At the southern end of Butte ridge, a succession of polymictic conglomerate with alkalic volcanic clasts (uTrSvc.gal) transitions westward into unassigned volcanic rocks (uTrSv; Fig. 3c); the contact is not exposed. The unassigned volcanic rocks include medium grey lapillistone to tuff breccia with volcanic clasts that contain 15-20% equant mafic minerals (1 mm). Farther west, across the axial trace of an inferred synform, the lapillistone to tuff breccia succession envelops

43

Geological Fieldwork 2022, British Columbia Ministry of Energy, Mines and Low Carbon Innovation, British Columbia Geological Survey Paper 2023-01

Fig. 16. Foliated polymictic conglomerate interbedded with sandstone to coarse crystal tuff, south end of Butte ridge, unit uTrSvc.gal (UTM 348945E–6332394N).

distinct dark green fragmental volcanic rocks with ~10% mafic minerals (<1 mm, Fig. 3c).

4.2. Galore plutonic suite (Late Triassic)

A multi-phase syenitic to monzodioritic intrusive complex in the Galore Creek valley (Fig. 2) envelopes and partly hosts the mineral deposits in the area. The alkalic intrusions typically contain distinct K-feldspar phenocrysts and/or pseudoleucite phenocrysts. Numerous smaller satellite stocks, sills, and dikes are present throughout the Galore Creek area. The intrusive phases were not studied in detail here, and the reader is referred to Enns et al. (1995) for detailed descriptions.

In the Copper canyon area, common K-feldspar- and pseudoleucite-K-feldspar-phyric intrusions cut all units, including the K-feldspar-phyric volcanic unit (uTrSv.xor). Two distinct pyritic pseudoleucite and K-feldspar porphyritic dikes (up to 1 m wide) were observed cutting unit uTrSv.xor. These dikes may be related to a compositionally similar stock centred on the Copper canyon deposit (Petsel and McConeghy, 2008; Fig. 2). At the southeast end of Butte ridge in drill hole GCT-21-009, several Galore intrusions cut the pseudoleucite-phyric volcanic unit (uTrSv.xlct; Figs. 3c, 7), and include fine-grained equigranular and K-feldspar porphyritic varieties.

5. Geochronology

Herein we present preliminary results for four geochronology samples collected in 2019. Detailed analytical methods and final results will be reported elsewhere. U-Pb zircon and titanite analyses were carried out at the Pacific Centre for Isotopic and Geochemical Research (University of British Columbia), and Ar-Ar biotite analyses at the Manitoba Isotope Research Facility (University of Manitoba). Two samples failed to return zircon or titanite: one sample of the K-feldspar-phyric volcanic unit (19BvS-9-84, UTM 357008E-6334238N); and one sample

of the pseudoleucite-phyric volcanic unit (19BvS-9-80, UTM 348679E-6333727N).

5.1. Biotite-phyric volcanic unit (uTrSv.xbt), upper succession

In the Copper canyon area, near the top of the biotite-phyric volcanic unit (uTrSv.xbt), we sampled a green-weathering well-stratified coarse crystal tuff, lapilli tuff, and volcanic sandstone (Figs. 2, 7; sample 19BvS-9-83, UTM 357039E-6334294N). The rocks contain abundant fresh biotite (0.5-2 mm), common angular K-feldspar crystals, and angular to subangular biotite-phyric and K-feldspar-phyric volcanic clasts. The sample returned a 209 ±1 Ma Ar-Ar biotite cooling age defined by 86.62% of [39]Ar released (Fig. 17a). Heating steps 3 to 6 define a visual plateau, and because the errors on the dates for these steps are very small (0.2 Ma at 2σ, Fig. 17a), we report the two sigma error on the age as the standard deviation of the dates for these steps.

5.2. K-feldspar-phyric volcanic unit (uTrSv.xor), upper succession

At the north end of Butte ridge, from the immediate base of the K-feldspar-phyric volcanic unit (uTrSv.xor), we sampled interstratified coarse crystal tuff, lapilli-tuff, lapillistone, and minor tuff or fine-grained volcanic-derived sandstone (Figs. 2, 7; sample 19BvS-9-82, UTM 348565E-6334285N). The outcrop contains abundant K-feldspar-phyric volcanic clasts set in a K-feldspar crystal-rich matrix, with rare 30-40 cm sandstone clasts. The sample yielded minor zircon and titanite. It returned a U-Pb zircon chemical abrasion thermal ionization mass spectrometry (CA-TIMS) date of 210.27 ±0.19 Ma, an overlapping U-Pb titanite isotope dilution thermal ionization mass spectrometry (ID TIMS) date of 210.22 ±0.36 Ma, and a combined 210.26 ±0.17 Ma date (Fig. 17b) interpreted as the depositional age. It is the first precise age determination for the onset of upper succession alkalic volcanism in northwestern British Columbia.

6. Discussion

Below we present thickness estimates and discuss the general depositional setting, volcanic history, and significance of intermediate volcanic and alkalic volcanic rocks of the Stuhini Group in the Galore Creek area, and the tectonic setting of Stuhini Group volcanism regionally.

6.1. Thickness estimates

In Figure 18 we compare the thickness estimates of the Stuhini Group at Butte ridge and Copper canyon area with those for the Central zone deposit area (L. Bailey, pers. comm., 2022). The Central zone estimates are based on a three-dimensional lithological model generated from extensive drilling of altered and mineralized rocks. Thickness estimates at Butte ridge and the Copper canyon area have been corrected by removing intrusions and subvolcanic sills. Due to strong texturally

44

Geological Fieldwork 2022, British Columbia Ministry of Energy, Mines and Low Carbon Innovation, British Columbia Geological Survey Paper 2023-01
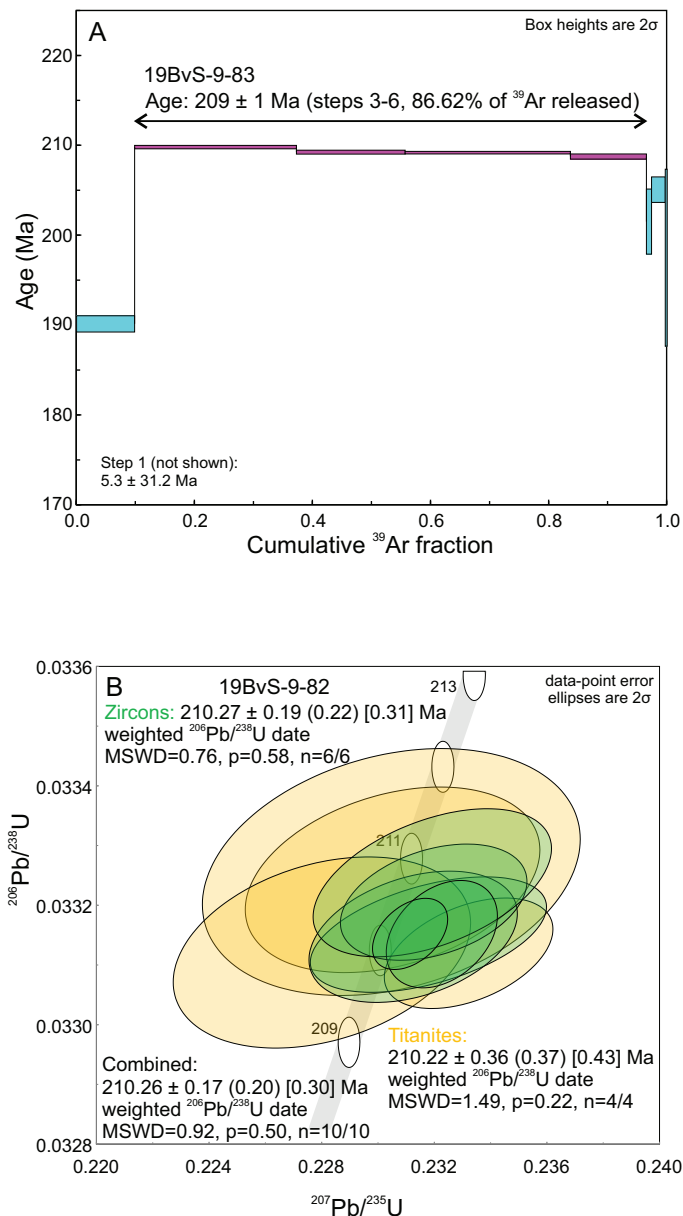
Fig. 17. Geochronology plots. **a)** Biotite Ar-Ar step-heating spectrum from biotite-phyric volcanic unit (uTrSv.xbt). **b)** U-Pb concordia diagram showing zircon CA-TIMS and titanite ID-TIMS results from the base of the K-feldspar-phyric volcanic unit (uTrSv.xor). Weighted average 2σ errors are reported in the format ±X (Y) [Z] of Schoene et al. (2006), where X is based on analytical errors only; Y also includes isotopic tracer errors, and Z also includes analytical, tracer and ^{238}U decay constant errors. When comparing U-Pb results with dates derived from other isotopic systems (e.g., Ar-Ar), the largest error, Z, should be used.

destructive hydrothermal alteration and mineralization, it is unclear if the pseudoleucite-phyric unit in the Central zone represents a subvolcanic intrusion, an extrusive volcanic unit, or a combination of both (L. Bailey, N. Peterson and W.-S. Lee, pers. comm., 2022).

Precise thickness estimates for Butte ridge and the Copper canyon area are hampered by common massive to poorly

stratified lithological units, tectonic flattening fabrics, folds, and faults. The thickness estimates for the southeast end of Butte ridge may be overestimated due to limited bedding measurements and possible folds. At the north end of Butte ridge, thickness estimates may be underestimated due to the flattening fabric developed throughout the area. Thickness estimates for the Copper canyon area may be overestimated because of unrecognized folds. Minimum thickness estimates for the lower intermediate to mafic volcano-sedimentary succession vary from 0.7 km at Butte ridge, to 1.1 km in the Central zone, to 1.8 km in the Copper canyon area and suggest an eastward thickening trend (Fig. 18). The average of these three measurements, 1.2 km, is probably a realistic minimum for this succession. The upper alkalic volcanic succession shows significant facies changes throughout the Galore Creek area but is at least 0.8 km thick.

6.2. Depositional setting and volcanic history

The lower intermediate to mafic volcano-sedimentary succession grades upward from a conglomeratic unit containing hornblende-phyric intermediate volcanic clasts and augite-phyric mafic volcanic clasts, a finer-grained sedimentary unit capped by limestone, a mafic volcanic unit to a feldspathoid-bearing mafic volcanic unit. Abundant coarse volcanic clasts in the lower conglomeratic unit suggests proximity to volcanic centres. The succession was deposited, at least in part, in a submarine setting as shown by the presence of marine bivalves, corals, and limestone. A fining upward trend accompanied by a decrease in volcanic debris in the sedimentary unit (Fig. 7) likely marks the decline of intermediate volcanic activity culminating in limestone deposition. The overlying mafic volcanic and feldspathoid-bearing mafic volcanic units are largely primary volcanic in origin, with limited evidence for reworking and very rare sandy limestone beds suggesting possible continued subaqueous deposition. The presence of monomictic volcanic breccia with feldspathoid-augite-phyric volcanic clasts up to 1 m (unit uTrSvm.xanl) in the Copper canyon area suggests vent-proximal deposition, and a transition to silica-undersaturated magmatism.

The upper alkalic volcanic succession includes a biotite-phyric volcanic unit, a K-felspar-phyric volcanic unit, pseudoleucite-phyric volcanic and subvolcanic units and a polymictic conglomerate unit with alkalic volcanic clasts. A sharp basal contact suggests an abrupt change to alkalic volcanism. In the Copper canyon area, initial deposition occurred in a subaqueous setting with common sedimentary rocks and reworked biotite crystal-rich volcanic strata (both containing soft-sediment deformation structures) near the base grading up into biotite-phyric volcanic rocks. Accretionary lapilli near the top of this unit at the toe of the Copper canyon glacier suggest a change to subaerial deposition. This unit has not been observed in the Galore Creek valley and on Butte ridge. Within the overlying K-feldspar-phyric unit, accretionary lapilli, welded beds, and irregular-shaped bombs suggest subaerial primary volcanic deposition. This unit is observed throughout the Galore Creek

45

Geological Fieldwork 2022, British Columbia Ministry of Energy, Mines and Low Carbon Innovation, British Columbia Geological Survey Paper 2023-01
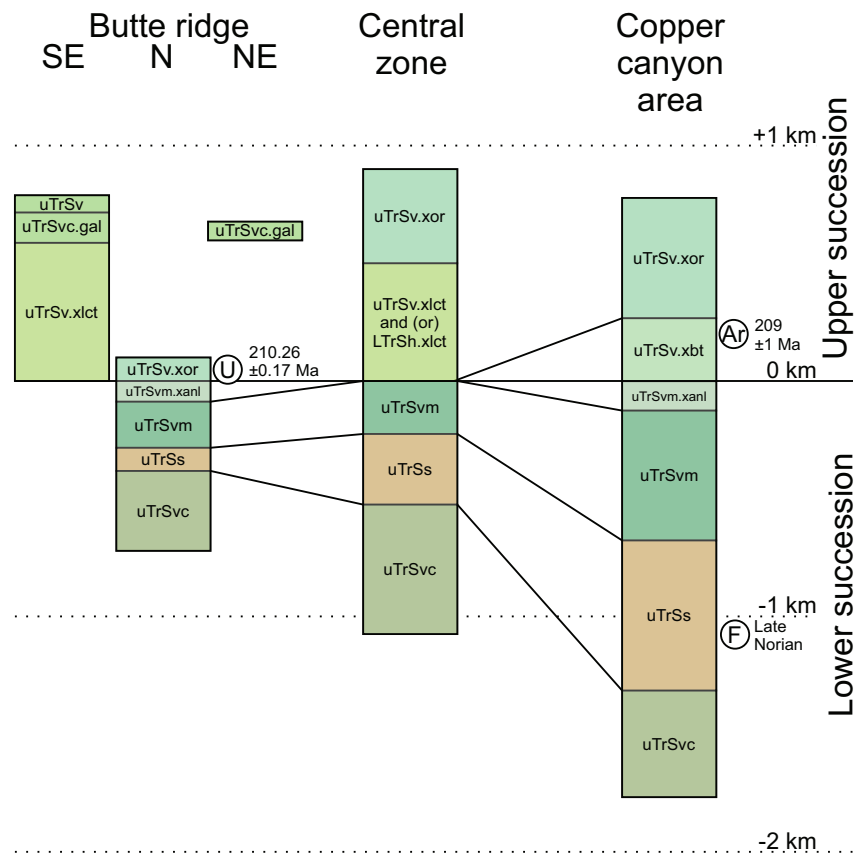
Fig. 18. Stratigraphic thickness variations and correlations across the Galore Creek district from west to east. Thicknesses are corrected by removing (subvolcanic) intrusions. Central zone deposit area thicknesses from L. Bailey (pers. comm., 2022).

area, suggesting a paleogeography with an emergent volcanic centre. A pseudoleucite-phyric volcanic unit several 100 m thick is at the south end of Butte ridge, with unknown thicknesses of pseudoleucite-phyric volcanic rocks at the east end of Butte ridge. A thick section of pseudoleucite-phyric rocks also occurs in the Central zone, but their origin as volcanic and/or subvolcanic rocks is uncertain due to a strong alteration and mineralization overprint. Their absence in the eastern part of the study area suggests they formed local volcanic centres. The relative timing of K-feldspar-phyric and pseudoleucite-phyric volcanism is uncertain. They may be temporally coincident but spatially restricted, temporally coincident and interfingering, or superimposed. Polymictic conglomerates from reworking of alkalic volcanic strata on Butte ridge either formed late or in a more distal position that allowed sourcing from different volcanic centres. No strata younger than the alkalic volcanic succession have been observed in the study area, and the lack of a top contact precludes determination of total thicknesses.

6.3. Stuhini Group intermediate volcanic rocks

Throughout Stikinia, Lewes River, Stuhini and Takla group (Late Triassic) volcanic strata consist predominantly of augite-phyric mafic volcanic rocks (Monger, 1977; Bradford and Brown, 1993; van Straaten et al., 2022). In contrast, Late Triassic strata in the Galore Creek area and west half

of the Telegraph Creek map sheet (NTS 104G/W, Fig. 1) contain both augite-phyric mafic volcanic and hornblende-phyric intermediate volcanic rocks (Logan and Koyanagi, 1994; Brown et al., 1996; this study). Interestingly, this area also exposes the oldest known rocks within Stikinia (Early to Middle Devonian Stikine assemblage; Logan et al., 2000; Logan, 2004) and the area contains two large (>1 Bt) porphyry Cu±Au deposits. The presence of intermediate volcanic rocks suggests a more mature arc segment, possibly due to a different crustal architecture or distinct magmatic evolution, which may have played a role in the region's significant endowment with magmatic-hydrothermal mineral deposits.

6.4. Stuhini Group alkalic volcanic rocks

Our high-precision U-Pb zircon and titanite age of 210.26 ±0.17 Ma for the onset of upper succession alkalic volcanism is broadly coeval with published ages for mineralogically, texturally, and compositionally similar alkalic silica-undersaturated Galore intrusions (ca. 210-208 Ma, see Section 2.2.) and genetically related porphyry Cu-Au-Ag formation. Regionally, strata similar to the upper alkalic volcanic unit of the Stuhini Group described herein are prospective for Galore Creek-style porphyry systems. In the Burgundy ridge area (Fig. 1) K-feldspar- and biotite-phyric volcanic rocks are surrounded by an apron of detrital biotite-

46

Geological Fieldwork 2022, British Columbia Ministry of Energy, Mines and Low Carbon Innovation, British Columbia Geological Survey Paper 2023-01

rich wacke (Mihalynuk et al., 2011; 2012). The Burgundy ridge prospect (MINFILE 104B 325) hosts skarn- and porphyry-style alteration in K-feldspar-porphyritic syenitic rocks, where drilling returned 91.26 m of 0.38% Cu, 0.3 g/t Au and 4.12 g/t Ag (Enduro Metals Corp., 2021). A sample from a megacrystic syenite intrusion returned a 207.8 ±2.7 Ma LA-ICP-MS U-Pb titanite age (Enduro Metals Corp., 2021). In the Trek area (Fig. 1), pseudoleucite-phyric volcanic rocks and K-feldspar- and pseudoleucite-porphyritic intrusions were reported by Close and Danz (2012). Drilling at the Trek north zone prospect (MINFILE 104G 022) returned 113.64 m of 0.25% Cu, 0.30 g/t Au, and 3.01 g/t Ag (Close and Danz, 2012). The Galore Creek, Copper Canyon, Trek, and Burgundy ridge occurrences may represent a northwest-southeast trending corridor containing Stuhini Group alkalic volcanic rocks, with enhanced prospectivity and increased preservation potential for Galore Creek-type porphyry systems.

6.5. Tectonic setting

Our stratigraphic and geochronological studies at Galore Creek confirm that Stuhini arc volcanism, widespread throughout Stikinia, is succeeded by local ca. 210-208 Ma alkalic silica-undersaturated magmatism. Post-subduction alkalic magmatism is coeval with a significant magmatic gap, a regional-scale unconformity and deformation attributed to the onset of collision between the Yukon-Tanana and Stikine terranes (Nelson and van Straaten, 2020; Nelson et al., 2022).

7. Conclusions

Our stratigraphic studies in the Galore Creek area show that the Stuhini Group can be subdivided in a lower intermediate to mafic volcano-sedimentary succession and an upper alkalic volcanic succession. The lower succession (at least ~1.2 km thick) shows a fining upward sequence from reworked intermediate ±mafic volcanic rocks to sedimentary rocks (Late Norian), which are overlain by mafic volcanic rocks and capped by a relatively thin unit of analcime-bearing mafic volcanic rocks. Deposition of the lower succession was, at least in part, submarine. The lower succession is part of the Stuhini arc found along the eastern margin and northern part of Stikinia.

The contact between the lower succession and the upper alkalic volcanic succession (at least ~0.8 km thick) is abrupt. In the east, a local biotite-phyric volcanic and reworked volcanic unit was largely deposited subaqueously. Overlying K-feldspar-phyric volcanic rocks are found throughout the Galore area and record subaerial deposition A thick package of pseudoleucite-phyric volcanic rocks and pseudoleucite-phyric subvolcanic intrusions is in the western and central parts of the Galore area; its depositional setting and relationships to other alkalic units are unclear. We constrain the onset of upper succession alkalic volcanism to 210.26 ±0.17 Ma using high-precision U-Pb zircon and titanite geochronology, broadly coeval with less-precise published ages for mineralogically, texturally, and compositionally similar alkalic silica-undersaturated Galore intrusions (ca. 210-208 Ma) suggesting a short-lived alkalic

magmatic event responsible for porphyry Cu-Au-Ag formation. The upper alkalic volcanic succession and alkalic silica-undersaturated Galore intrusions are part of a magmatic belt of small-volume stocks and rare volcanic rocks that orthogonally transects the earlier Stuhini arc. It reflects post-subduction alkalic magmatism and alkalic silica-undersaturated porphyry Cu-Au-Ag deposit formation during the early stages of Yukon-Tanana-Stikinia collision.

Acknowledgments

References cited

Allmendinger, R.W., Cardozo, N.C., and Fisher, D., 2013. Structural Geology Algorithms: Vectors and Tensors. Cambridge University Press, 289 p.

Bailey, L., and Jutras, G., 2016. 2015 assessment report on the Schaft Creek porphyry copper-gold-molybdenum deposit. British Columbia Ministry of Energy and Mines, British Columbia Geological Survey Assessment Report 35967, 107 p.

Bradford, J.A., and Brown, D.A., 1993. Geology of the Bearskin Lake and southern Tatsamenie Lake map areas, northwestern British Columbia (104K/1 and 8). In: Geological Fieldwork 1992, British Columbia Ministry of Energy and Mines, British Columbia Geological Survey Paper 1993-1, pp. 159-176.

Brown, D.A., Gunning, M.H., and Greig, C.J., 1996. The Stikine project: Geology of western Telegraph Creek map area, northwestern British Columbia. British Columbia Ministry of Employment and Investment, British Columbia Geological Survey Bulletin 95, 130 p.

Byrne, K., and Tosdal, R.M., 2014. Genesis of the Late Triassic southwest zone breccia-hosted alkalic porphyry Cu-Au deposit, Galore Creek, British Columbia, Canada. Economic Geology, 109, 915-938. Doi: 10.2113/econgeo.109.4.915.

Campbell, M.E., 2021. The geology and geochemistry of the Sulphurets district porphyry Au-Cu-Mo deposits, British Columbia, Canada: Insights from a long-lived, gold-enriched porphyry district. Ph.D. thesis, Oregon State University, 238 p. Available from <https://ir.library.oregonstate.edu/concern/graduate_thesis_or_dissertations/jw827k32f>

Cardozo, N., and Allmendinger, R.W., 2013. Spherical projections with OSXStereonet. Computers & Geosciences, 51, 193-205. Doi: 10.1016/j.cageo.2012.07.021.

Close, S., and Danz, N., 2012. 2011 Geological, geophysical and geochemical report on the Trek property. British Columbia Ministry of Energy and Mines, British Columbia Geological Survey Assessment Report 32866, 53 p.

Colpron, M., Sack, P.J., Crowley, J.L., Beranek, L.P., and Allan, M.M., 2022. Late Triassic to Jurassic magmatic and tectonic evolution of the intermontane terranes in Yukon, northern Canadian Cordillera: Transition from arc to syn-collisional magmatism and post-collisional lithospheric delamination. Tectonics, 41 (2), e2021tc007060. Doi: 10.1029/2021TC007060.

Coulson, I.M., Russell, J.K., and Dipple, G.M., 1999. Origins of the

47

Geological Fieldwork 2022, British Columbia Ministry of Energy, Mines and Low Carbon Innovation, British Columbia Geological Survey Paper 2023-01

Zippa Mountain pluton: a Late Triassic, arc-derived, ultrapotassic magma from the Canadian Cordillera. Canadian Journal of Earth Sciences, 36, 1415-1434. Doi: 10.1139/e99-045.

Cui, Y., Hickin, A.S., Schiarizza, P., and Diakow, L.J., 2017. British Columbia digital geology. British Columbia Ministry of Energy, Mines and Petroleum Resources, British Columbia Geological Survey Open File 2017-08, 9p. Data version 2019-12-19. <https://www2.gov.bc.ca/gov/content/industry/mineral-exploration-mining/british-columbia-geological-survey/geology/bcdigitalgeology>

Duuring, P., Rowins, S.M., McKinley, B.S.M., Dickinson, J.M., Diakow, L.J., Kim, Y.-S., and Creaser, R.A., 2009. Examining potential genetic links between Jurassic porphyry Cu-Au ±Mo and epithermal Au ±Ag mineralization in the Toodoggone district of north-central British Columbia, Canada. Mineralium Deposita, 44, 463-496. Doi: 10.1007/s00126-008-0228-9.

Enduro Metals Corp., 2021. University study pinpoints Enduro's Burgundy system as Galore Creek suite. News release, January 18, 2021. https://endurometals.com/ (last accessed December 16, 2022).

Enns, S.G., Thompson, J.F.H., Stanley, C.R., and Yarrow, E.W., 1995. The Galore Creek porphyry copper-gold deposits, northwestern British Columbia. In: Schroeter, T.G., (Ed.), Porphyry deposits of the northwestern Cordillera of North America, Canadian Institute of Mining and Metallurgy, Special Volume 46, pp. 630-644.

Evenchick, C.A., McMechan, M.E., McNicoll, V.J., and Carr, S.D., 2007. A synthesis of the Jurassic-Cretaceous tectonic evolution of the central and southeastern Canadian Cordillera: Exploring links across the orogen. In: Sears, J.W., Harms, T.A., and Evenchick, C.A., (Eds.), Whence the Mountains? Inquiries into the Evolution of Orogenic Systems: A Volume in Honor of Raymond A. Price, Geological Society of America Special Paper 433, 117-145. Doi: 10.1130/2007.2433(06).

Hatch Ltd., GR Technical Services Ltd., and Giroux Consultants Ltd., 2005. Geology and resource potential of the Copper canyon property. NI 43-101 technical report prepared for NovaGold Resources Inc., 74p. Available from <https://www.sedar.com>

Henderson, J.R., Kirkham, R.V., Henderson, M.N., Payne, J.G., Wright, T.O., and Wright, R.L., 1992. Stratigraphy and structure of the Sulphurets area, British Columbia. In: Current Research, Part A, Cordillera and Pacific Margin, Geological Survey of Canada, Paper no. 92-1A, pp. 323-332.

Hollis, L., and Bailey, L., 2013. Assessment report on drilling, geological, geochemical and geophysical work conducted during 2012 at the GJ/Kinaskan copper-gold porphyry project. BC Ministry of Energy and Mines, British Columbia Geological Survey Assessment Report 33815, 60 p.

Hunter, R.C., and van Straaten, B.I., 2020. Preliminary stratigraphy and geochronology of the Hazelton Group, Kitsault River area, Stikine terrane, northwest British Columbia. In: Geological Fieldwork 2019, British Columbia Ministry of Energy, Mines and Petroleum Resources, British Columbia Geological Survey Paper 2020-02, pp. 101-118.

Johnston, R., Kennedy, L., and van Straaten, B.I., 2023. Preliminary observations of a high-strain zone along the western flank of the Galore Creek deposit area, northwestern British Columbia. In: Geological Fieldwork 2022, British Columbia Ministry of Energy, Mines and Low Carbon Innovation, British Columbia Geological Survey Paper 2023-01, pp. 51-63.

Kovacs, N., Allan, M.M., Crowley, J.L., Colpron, M., Hart, C.J.R., Zagorevski, A., and Creaser, R.A., 2020. Carmacks copper Cu-Au-Ag deposit: Mineralization and postore migmatization of a Stikine arc porphyry copper system in Yukon, Canada. Economic Geology, 115, 1413-1442. Doi: 10.5382/econgeo.4756.

Lang, J.R., Stanley, C.R., and Thompson, J.F.H., 1995. Porphyry copper-gold deposits related to alkaline igneous rocks in the Triassic-Jurassic arc terranes of British Columbia. In: Pierce, F.W., and Bolm, J.G., (Eds.), Porphyry Deposits of the American Cordillera, Arizona Geological Society Digest 20, pp. 219-236.

Logan, J.M., 2004. Geology and geochemistry of the Foremore area. British Columbia Ministry of Energy and Mines, British Columbia Geological Survey Open File 2004-11, 1:50,000 scale.

Logan, J.M., Drobe, J.R., and McClelland, W.C., 2000. Geology of the Forrest Kerr-Mess Creek area, northwestern British Columbia. British Columbia Ministry of Energy and Mines, British Columbia Geological Survey Bulletin 104, 132 p.

Logan, J.M., and Koyanagi, V.M., 1994. Geology and mineral deposits of the Galore Creek area. British Columbia Ministry of Energy, Mines and Petroleum Resources, British Columbia Geological Survey Bulletin 92, 102 p.

Logan, J.M., and Mihalynuk, M.G., 2014. Tectonic controls on Early Mesozoic paired alkaline porphyry deposit belts (Cu-Au ±Ag-Pt-Pd-Mo) within the Canadian Cordillera. Economic Geology, 109, 827-858. Doi: 10.2113/econgeo.109.4.827.

Logan, J.M., Koyanagi, V.M., and Rhys, D., 1993a. Geology and mineral occurrences of the Galore Creek area (NTS 104G/3). British Columbia Ministry of Energy, Mines and Petroleum Resources, British Columbia Geological Survey Geoscience Map 1993-01. 1:50,000 scale.

Logan, J.M., Koyanagi, V.M., and Rhys, D., 1993b. Geology and mineral occurrences of the Galore Creek area (NTS 104G/4). British Columbia Ministry of Energy, Mines and Petroleum Resources, British Columbia Geological Survey Geoscience Map 1993-02. 1:50,000 scale.

Micko, J., Tosdal, R.M., Bissig, T., Chamberlain, C.M., and Simpson, K.A., 2014. Hydrothermal alteration and mineralization of the Galore Creek alkalic Cu-Au porphyry deposit, northwestern British Columbia, Canada. Economic Geology, 109, 891-914. Doi: 10.2113/econgeo.109.4.891.

Mihalynuk, M.G., Nelson, J., and Diakow, L.J., 1994. Cache Creek terrane entrapment: Oroclinal paradox within the Canadian Cordillera. Tectonics, 13, 575-595. Doi: 10.1029/93TC03492.

Mihalynuk, M.G., Logan, J.M., Zagorevski, A., and Joyce, N., 2011. Geology and mineralization of the Hoodoo Mountain area (NTS 104B/14E). In: Geological Fieldwork 2010, British Columbia Ministry of Energy and Mines, British Columbia Geological Survey Paper 2011-1, pp. 37-63.

Mihalynuk, M.G., Zagorevski, A., and Cordey, F., 2012. Geology of the Hoodoo Mountain area (NTS 104B/14W). In: Geological Fieldwork 2011, British Columbia Ministry of Energy and Mines, British Columbia Geological Survey Paper 2012-1, pp. 45-68.

Mihalynuk, M.G., Zagorevski, A., Joyce, N.L., and Creaser, R.A., 2016. Age of magmatism and mineralization at the Star (Sheslay, Copper Creek) copper porphyry prospect: Inception of the Late Triassic mineralized arc. In: Geological Fieldwork 2015, British Columbia Ministry of Energy and Mines, British Columbia Geological Survey Paper 2016-1, pp. 65-75.

Mihalynuk, M.G., Zagorevski, A., Logan, J.M., Friedman, R.M., and Johnston, S.T., 2019. Age constraints for rocks hosting massive sulphide mineralization at Rock and Roll and Granduc deposits between Iskut and Stewart, British Columbia. In: Geological Fieldwork 2018, Ministry of Energy, Mines and Petroleum Resources, British Columbia Geological Survey Paper 2019-01, pp. 97-111.

Monger, J.W.H., 1977. The Triassic Takla Group in McConnell Creek map-area, north central British Columbia. Geological Survey of Canada, Paper 76-29, 45 p.

Mortensen, J.K., Ghosh, D., and Ferri, F., 1995. U-Pb age constraints of intrusive rocks associated with copper-gold porphyry deposits in the Canadian Cordillera. In: Schroeter, T.G., (Ed.), Porphyry Deposits of the Northwestern Cordillera of North America, Canadian Institute of Mining and Metallurgy Special Volume 46, pp. 142-158.

Nelson, J.L., Colpron, M., and Israel, S., 2013. The Cordillera of British Columbia, Yukon and Alaska: Tectonics and metallogeny.

48

Geological Fieldwork 2022, British Columbia Ministry of Energy, Mines and Low Carbon Innovation, British Columbia Geological Survey Paper 2023-01

In: Colpron, M., Bissig, T., Rusk, B. G., and Thompson, J., (Eds.), Tectonics, Metallogeny and Discovery: The North American Cordillera and Similar Accretionary Settings, Society of Economic Geologists Special Publication 17, pp. 53-110.

Nelson, J.L., and van Straaten, B.I., 2020. Recurrent syn- to post-subduction mineralization along deep crustal corridors in the Iskut-Stewart-Kitsault region of western Stikinia, northwestern British Columbia. In: Sharman, E.R., Lang, J.R., and Chapman, J.B., (Eds.), Porphyry Deposits of the Northwestern Cordillera of North America: A 25-Year Update, Canadian Institute of Mining and Metallurgy Special Volume 57, pp. 149-211.

Nelson, J.L., van Straaten, B., and Friedman, R., 2022. Latest Triassic-Early Jurassic Stikine-Yukon-Tanana terrane collision and the onset of accretion in the Canadian Cordillera: Insights from Hazelton Group detrital zircon provenance and arc-back-arc configuration. Geosphere, 18, 670-696. Doi: 10.1130/GES02444.1.

Nelson, J.L., Waldron, J., van Straaten, B.I., Zagorevski, A., and Rees, C., 2018. Revised stratigraphy of the Hazelton Group in the Iskut River region, northwestern British Columbia. In: Geological Fieldwork 2017, British Columbia Ministry of Energy, Mines and Petroleum Resources, British Columbia Geological Survey Paper 2018-1, pp. 15-38.

Oliver, J., and Gabites, J., 1993. Geochronology of rocks and polyphase deformation, Bearskin (Muddy) and Tatsamenie lakes district, northwestern British Columbia (104K/8, 1). In: Geological Fieldwork 1992, British Columbia Ministry of Energy, Mines and Natural Gas, British Columbia Geological Survey Paper 1993-1, pp. 177-188.

Petsel, S.A., and McConeghy, C., 2008. 2007 Diamond drilling assessment report on the Copper canyon property. British Columbia Ministry of Energy and Mines, British Columbia Geological Survey Assessment Report 30184, 21 p.

Prince, J., 2020. 2019 drilling, geological mapping and aerial survey assessment report on the Galore Creek project. British Columbia Ministry of Energy and Mines, British Columbia Geological Survey Assessment Report 39156, 48 p.

Rees, C., Riedell, K.B., Proffett, J.M., Macpherson, J., and Robertson, S., 2015. The Red Chris porphyry copper-gold deposit, northern British Columbia, Canada: Igneous phases, alteration, and controls of mineralization. Economic Geology, 110, 857-888. Doi: 10.2113/econgeo.110.4.857.

Rhys, D.A., 1993. Geology of the Snip mine, and its relationship to the magmatic and deformational history of the Johnny Mountain area, northwestern British Columbia. M.Sc. thesis, The University of British Columbia, Vancouver, B.C., Canada. <https://circle.ubc.ca/handle/2429/2173>

Schoene, B.A., Crowley, J.L., Condon, D.J., Schmitz, M.D., and Bowring, S.A., 2006. Reassessing the uranium decay constants for geochronology using ID-TIMS U-Pb data. Geochimica et Cosmochimica Acta, 70 (2006), 426-445.

Schwab, D.L., Petsel, S., Otto, B.R., Morris, S.K., Workman, E.E., and Tosdal, R.M., 2008. Overview of the Late Triassic Galore Creek copper-gold-silver porphyry system, northwestern British Columbia, Canada. In: Spencer, J. E., and Titley, S R., (Eds.), Ores and Orogenesis: Circum-Pacific Tectonics, Geologic Evolution and Ore Deposits, Arizona Geological Society Digest 22, pp. 471-484.

Scott, J.E., Richards, J.P., Heaman, L.M., Creaser, R.A., and Salazar, G.S., 2008. The Schaft Creek porphyry Cu-Mo-(Au) deposit, northwestern British Columbia. Exploration and Mining Geology, 17, 163-196. Doi: 10.2113/gsemg.17.3-4.163.

Teck Resources Limited, 2019. Annual information form. Report by Teck Resources Limited, 121 p. Available from <https://www.sedar.com/>

van Straaten, B.I., Logan, J.M., and Diakow, L.J., 2012. Mesozoic magmatism and metallogeny of the Hotailuh batholith, northwestern British Columbia. British Columbia Ministry of Energy, Mines and Natural Gas, British Columbia Geological Survey Open File 2012-06, 58 p.

van Straaten, B.I., Logan, J.M., Nelson, J.L., Moynihan, D.P., Diakow, L.J., Gibson, R., Bichlmaier, S.J., Wearmouth, C.D., Friedman, R.M., Golding, M.L., Miller, E.A., and Poulton, T.P., 2022. Bedrock geology of the Dease Lake area. British Columbia Ministry of Energy, Mines and Low Carbon Innovation, British Columbia Geological Survey Geoscience Map 2022-01, 1:100,000 scale.

Yukon Geological Survey, 2018. Yukon digital bedrock geology. Yukon Geological Survey. Available from <https://data.geology.gov.yk.ca/Compilation/3>